COMMUNICATION

ChemComm
www.rsc.org/chemcomm

C–H···π interactions in the low-temperature crystal structures of α,ω-unsaturated linear hydrocarbons†

Andrew D. Bond
University of Cambridge, Department of Chemistry, Lensfield Road, Cambridge UK CB2 1EW.
E-mail: adb29@cam.ac.uk

Received (in Cambridge, UK) 8th May 2002, Accepted 26th June 2002
First published as an Advance Article on the web 9th July 2002

The low-temperature crystal structures of 1,7-octadiene (C_8H_{14}), 1,9-decadiene ($C_{10}H_{18}$), 1,7-octadiyne (C_8H_{10}) and 1,9-decadiyne ($C_{10}H_{14}$), determined following *in situ* crystal growth from the liquid, reveal the role of C–H···π interactions in α,ω-unsaturated linear hydrocarbons in the solid state.

The nature of intermolecular interactions in the solid state is often exemplified by the crystal structures of the hydrocarbons.[1] A recent report of the low-temperature crystal structures of the *n*-alkanes, for example, reveals the origin of the odd–even alternation in their melting points: the melting point is correlated with alternating crystal density that arises from less dense packing of the odd members of the series.[2] In hydrocarbons incorporating alkyne and alkene groups, interactions of the type C–H···π are evident. The low-temperature crystal structures of ethyne (C_2H_2) and ethene (C_2H_4), for example, contain networks of C–H···π interactions at near-linear geometry.[3,4] Database studies suggest that these interactions display directional characteristics comparable with weak hydrogen bonds, in which the C–H groups target the midpoint of the C≡C or C=C bond, or are slightly displaced towards the terminal C atom.[5,6] Computational studies of the C–H···π interaction indicate that in addition to dispersion forces, electrostatic and charge-transfer (π–σ*) components contribute to the overall interaction energy.[7,8] Comparative examination of C–H···π interactions in small unsaturated (non-aromatic) hydrocarbons is hindered by the fact that they are generally liquids or gases at room temperature. Recent advances in instrumentation and techniques for *in situ* crystal growth of low-melting materials, however, are beginning to facilitate determination of the crystal structures of the most basic molecules,[9] aiding elucidation of the fundamental nature of weak interactions in the solid state. Reported here are the low-temperature crystal structures of the α,ω-alkyldienes, 1,7-octadiene **1** and 1,9-decadiene **2**, and the α,ω-alkyldiynes, 1,7-octadiyne **3** and 1,9-decadiyne **4**, the first terminally-unsaturated linear hydrocarbons to be examined successfully by X-ray crystallography. The structures, determined following *in situ* crystal growth from the liquid,‡ reveal the role of C–H···π interactions in determining the structures and physical properties of these molecules in the solid state.

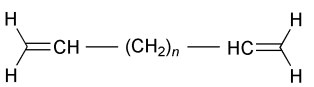

1 $n = 4$
2 $n = 6$

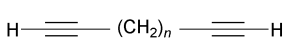

3 $n = 4$
4 $n = 6$

Dienes **1** and **2** adopt layered structures, in which the axes of the central $(CH_2)_n$ chains run normal to the plane of the layers, and close to parallel in all molecules, an arrangement similar to that observed in the *n*-alkanes (Fig. 1). The angle between molecular axes in adjacent molecules within a layer is minimal for **2** (1.1°), and slightly larger for **1** (3.5°). The terminal alkene groups form a herring-bone arrangement, giving rise to a network of C–H···π contacts (denoted (i) in Fig. 1) with angles to the mid-point of the C=C bond of 156.1 and 154.9° in **1** and **2**, respectively, and H···mid-point distances of 3.10 and 3.14 Å, respectively. Somewhat longer C–H···π contacts also exist (denoted (ii) in Fig. 1) in which the C–H group adopts a bifurcated arrangement (C–H···mid-point *ca.* 122°, 3.30 Å and 141°, 3.57 Å). The C–H···π networks are essentially identical in **1** and **2**, and the *b* and *c* lattice parameters are comparable in the two structures. The *a* lattice parameter shows an increase of *ca.* 2.3 Å with increasing alkyl chain length, corresponding to the expected 2.54 Å increase along the molecular axis.

Diynes **3** and **4** also adopt layered structures in which the molecular axes are close to parallel, the deviation from co-linearity being 3.7° for **3** and 1.2° for **4**. In contrast to the *n*-alkanes and α,ω-dienes, however, an angle of *ca.* 117° is formed in the *bc* plane between the axes of molecules in adjacent layers (Fig. 2). This observation is significant, and arises from the herring-bone arrangement of the alkyne groups at the molecular termini. Each terminal H atom in **3** and **4** forms two C–H···π contacts in a bifurcated arrangement (Fig. 2). In **3**, the interaction angles (taken to the mid-point of the C≡C bond) are 129.0 and 131.5°, with H···mid-point distances of 2.99 and 3.02 Å, respectively. In **4**, the interaction angles are 126.7 and 133.6°, with H···mid-point distances of 3.03 and 3.01 Å, respectively. The C–H···π networks are essentially identical in **3** and **4**, and the *a* and *b* lattice parameters are comparable in the two structures. The *c* parameter shows an increase of *ca.* 4.5 Å

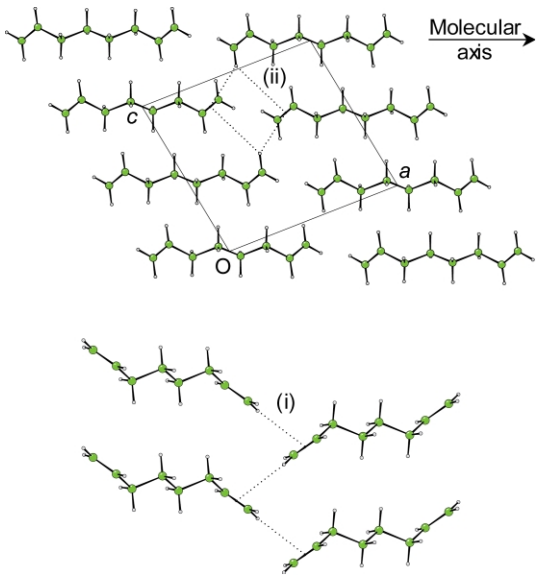

Fig. 1 Projection of **1** along the *b* direction (top), showing selected C–H···π contacts, and along the perpendicular direction (bottom), showing the herring-bone arrangement between terminal alkene groups. The direction of the molecular axes (normal to the close-packed layers) is indicated. The structure of **2** is comparable.

† Electronic supplementary (ESI) information available: experimental details of crystal growth for **1**–**4**, lattice-energy calculations for **1**–**4** and the *n*-alkanes, and definition and determination of the planar packing densities. See http://www.rsc.org/suppdata/cc/b2/b204261d/

DOI: 10.1039/b204261d

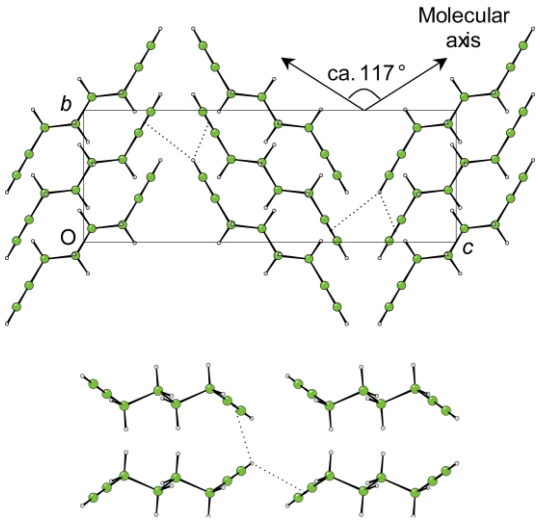

Fig. 2 Projection of **3** along the *a* direction showing the herring-bone arrangement of the terminal alkyne groups and selected C–H···π contacts (top). A single bifurcated arrangement is shown from the perpendicular direction (bottom). The structure of **4** is comparable.

with increasing alkyl chain length, again corresponding to the expected 2.54 Å increase per molecule along the molecular axis.

The influence of the C–H···π interactions in the structures of **1**–**4** may be assessed by comparison with the analogous alkanes, *n*-octane[2] and *n*-decane,[10] which adopt layered structures within which all molecular axes are parallel. Projection of the *n*-alkane layers onto the plane normal to the molecular axes reveals a primitive oblique subcell (Fig. 3) with dimensions $a_0 \approx 4.7$, $b_0 \approx 4.0$ Å and $\gamma_0 \approx 107°$. A similar projection of **1** and **2** reveals a rectangular subcell with dimensions $a_0 = 4.91$, $b_0 = 7.34$ Å for **1** and $a_0 = 4.90$, $b_0 = 7.27$ Å for **2** (Fig. 3). A rectangular subcell is also observed in **3** and **4**, with dimensions $a_0 = 4.98$, $b_0 = 7.06$ Å for **3**, and $a_0 = 5.04$, $b_0 = 7.08$ Å for **4**.† The observation of rectangular rather than oblique subcells in **1**–**4** (and also the fact that the molecular axes are not aligned exactly co-linearly) is a direct result of the geometry of the interactions between the molecular termini: the rectangular subcell accommodates the herring-bone geometry between the alkene groups in **1** and **2**, and the alkyne groups in **3** and **4**. The area per alkyl chain in the planar projections is 18.0, 17.8, 17.6 and 17.9 Å^2 for **1**–**4**, respectively, compared with 18.1 and 17.9 Å^2 for *n*-octane and *n*-decane. These values illustrate that despite the subtle change in packing arrangement within layers, the $(CH_2)_n$ chains remain essentially close-packed.

The total magnitude of the intermolecular dispersion forces in the structures may be expressed simply in terms of the lattice binding energy calculated using an empirical (6-12) van der Waals expression. The energies calculated in this manner are −69.3, −89.3, −61.6 and −79.4 kJ mol^{-1}, for **1**–**4** respectively, and −78.7 and −97.7 kJ mol^{-1} for *n*-octane and *n*-decane.[11]† For a given value of *n*, the total magnitude of the dispersion forces decreases in the order: alkane > α,ω-diene > α,ω-diyne. These values clearly are not correlated with the melting points of the materials,[12] however, which decrease for a given value of *n* in the order: α,ω-diyne > alkane > α,ω-diene. Since the entropy of melting is unlikely to differ significantly across the series, the trend in melting points reveals a substantial non-dispersive contribution from C–H···π interactions to the lattice energies of **3** and **4**. This contribution (which may comprise both electrostatic and charge-transfer components) is sufficient to offset the overall reduction in dispersion forces, such that the melting points of the α,ω-diynes are greater than those of the comparable *n*-alkanes. Any non-dispersive contribution from C–H···π interactions in **1** and **2** is clearly less significant than that in **3** and **4**, and the melting points of the α,ω-dienes are lower than those of the *n*-alkanes. This result displays gratifying agreement with previous observations that the magnitude of C–H···π interactions diminishes in line with the decreasing magnitude of the C–H dipole.[5,6]

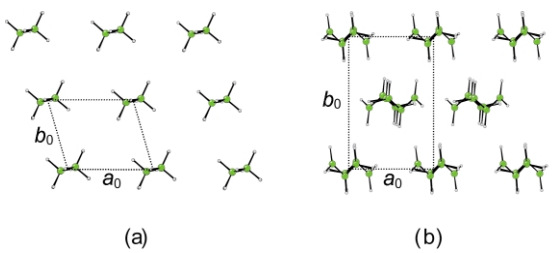

Fig. 3 Representative projections onto the plane normal to the molecular axes for single layers in the *n*-alkanes (a) and **1**-**4** (b). The oblique and rectangular subcells are indicated.

I am grateful to the EPSRC for financial support, and to Dr John E. Davies (University of Cambridge) for assistance with crystal growth and calculation of the planar packing densities.

Notes and references

‡ *Crystal data for* **1**: C_8H_{14}, $M = 110.19$, monoclinic, space group $P2_1/c$, $a = 9.3210(16)$, $b = 4.9140(5)$, $c = 8.7545(15)$ Å, $\beta = 99.510(6)°$, $U = 395.47(10)$ Å^3, $Z = 2$, $D_c = 0.925$ g cm^{-3}, μ(Mo-Kα) = 0.051 mm^{-1}. Of 1752 reflections measured, 620 were unique ($R_{int} = 0.0425$) and were used in all calculations. The final $wR2 = 0.1328$ (all data), $R1$ [$F^2 > 2\sigma(F^2)$] = 0.0476, and goodness-of-fit on F^2, $S = 1.07$ (CCDC 183117). *Crystal data for* **2**: $C_{10}H_{18}$, $M = 138.24$, monoclinic, space group $P2_1/c$, $a = 11.648(2)$, $b = 4.9005(8)$, $c = 8.819(1)$ Å, $= 105.31(1)°$, $U = 485.53(13)$ Å^3, $Z = 2$, $D_c = 0.946$ g cm^{-3}, μ(Mo-Kα) = 0.052 mm^{-1}. Of 3444 reflections measured, 1091 were unique ($R_{int} = 0.1830$) and were used in all calculations. The diffraction pattern clearly contained contributions from more than one crystal (reflected in the relatively high R_{int}), but only those associated with the major component were included in the integration. The final $wR2 = 0.2366$ (all data), $R1$ [$F^2 > 2\sigma(F^2)$] = 0.0763, and goodness-of-fit on F^2, $S = 1.13$ (CCDC 183118). *Crystal data for* **3**: C_8H_{10}, $M = 106.16$, orthorhombic, space group *Pbca*, $a = 7.0594(2)$, $b = 5.9531(2)$, $c = 16.7430(6)$ Å, $U = 703.63(4)$ Å^3, $Z = 4$, $D_c = 1.002$ g cm^{-3}, μ(Mo-Kα) = 0.056 mm^{-1}. Of 1086 reflections measured, 609 were unique ($R_{int} = 0.0105$) and were used in all calculations. The final $wR2 = 0.0947$ (all data), $R1$ [$F^2 > 2\sigma(F^2)$] = 0.0325, and goodness-of-fit on F^2, $S = 1.14$ (CCDC 183119). *Crystal data for* **4**: $C_{10}H_{14}$, $M = 134.21$, orthorhombic, space group *Pbca*, $a = 7.0832(3)$, $b = 5.9177(3)$, $c = 21.2692(11)$ Å, $U = 891.53(7)$ Å^3, $Z = 4$, $D_c = 1.000$ g cm^{-3}, μ(Mo-Kα) = 0.056 mm^{-1}. Of 2187 reflections measured, 1273 were unique ($R_{int} = 0.0266$) and were used in all calculations. The final $wR2 = 0.1294$ (all data), $R1$ [$F^2 > 2\sigma(F^2)$] = 0.0446, and goodness-of-fit on F^2, $S = 1.04$ (CCDC 183120). See http://www.rsc.org/suppdata/cc/b2/b204261d/ for crystallographic files in .cif or other electronic format.

1 A. I. Kitaigorodskii, *Molecular Crystals and Molecules*, Academic Press, New York, 1973.
2 R. Boese, H.-C. Weiss and D. Bläser, *Angew Chem., Int. Ed.*, 1999, **38**, 988.
3 G. J. H. van Nes and A. Vos, *Acta Crystallogr., Sect. B*, 1979, **35**, 2593.
4 R. K. McMullan, A. Kvick and P. Popelier, *Acta Crystallogr., Sect. B*, 1992, **48**, 726. The structure of ethene is actually that of the deuterated derivative C_2D_2, determined by neutron diffraction.
5 G. R. Desiraju and T. Steiner, *The Weak Hydrogen Bond in Structural Chemistry and Biology*, Oxford University Press, New York, 1999.
6 M. Nishio, M. Hirota and Y. Umezawa, *The CH/π Interaction,* Wiley-VCH, New York, 1998.
7 T. Takagi, A. Tanaka, S. Matsuo, H. Maezaki, M. Tani and H. Fujiwara and Y. Sasaki, *J. Chem. Soc., Perkin Trans. 2*, 1987, 1015.
8 M.-F. Fan, Z. Lin, J. E. McGrady and D. M. P. Mingos, *J. Chem. Soc., Perkin Trans. 2*, 1996, 563.
9 In addition to laser-assisted crystallisation techniques exemplified by reference 2, several recent successes have been reported using a simple zone-refinement method, described in: J. E. Davies and A. D. Bond, *Acta Crystallogr., Sect. E*, 2001, **57**, o947.
10 A. D. Bond and J. E. Davies, *Acta Crystallogr., Sect. E*, 2002, **58**, o196.
11 Lattice binding energies calculated in this way mirror the odd–even alternation in melting points for the *n*-alkanes (see ESI†).
12 Melting points (K): 1,7-octadiyne (241), *n*-octane (216), 1,7-octadiene (162); 1,9-decadiyne (263), *n*-decane (243), 1-9-decadiene (196).